Trauma Case Reports 46 (2023) 100848

Contents lists available at ScienceDirect

Trauma Case Reports

journal homepage: www.elsevier.com/locate/tcr

Case Report

The use of 3D printing technology in limb reconstruction. Inspirations and challenges

Efthymios Iliopoulos [a,*], Konstantinos Makiev [a], Paraskevas Georgoulas [a], Nick Vordos [b], Athanasios Ververidis [a], Konstantinos Tilkeridis [a]

[a] Trauma and Orthopaedics Department, Alexandroupolis University Hospital, University of Thrace, Alexandroupolis, Greece
[b] Biophysics Laboratory, Physics Department, International Hellenic University, Kavala, Greece

ARTICLE INFO

Keywords:
Three dimension printing
Septic non-union
Ankle arthrodesis
Bone transport

ABSTRACT

The management of septic non-unions with associated bone necrosis is challenging, especially when the resulting bone defect after the debridement is extensile. Different techniques have been described in the literature for the treatment of these demanding cases, with the most prominent being free vascularized Fibular graft and bone transport with distraction osteogenesis principles. Recently, 3D printing technology has been increasingly utilized in many complex orthopaedic pathologies. However, the application of those advancements regarding septic non-unions with residual bone defect has not been previously studied. This study presents a novel 3D printing technique for the management of an infected critical bone deficit of the tibia. Queries, challenges and future perspectives concerning the recruiting of 3D printing technology in limb reconstruction are also being discussed.

Clinical Evidence Level: IV.

Background

Septic non-union is defined as the lack of biological bone healing procedure and associated with local, persistent chronic infection [1]. Infected non-unions of tibia are especially problematic due to factors such as difficult-to-control infection, compound deformities, sclerotic bone ends, massive bone gaps, limb shortening, and joint dysfunction, some of them caused by multiple unsuccessful previous treatments [1].

Overall management of septic non-union of the distal tibia is considered to be demanding due to the complexity of the diverse available treatments which are inconsistent in terms of effectiveness. Both free vascularized fibular graft (FVFG) and Ilizarov bone transport (IBT) are effective reconstruction techniques for infected bone gaps of the lower limbs [2]. Additionally, the induced membrane (IM) technique (Masquelet) is another, 2 stages, restoring treatment for sites of critical bone deficits with high quality outcomes [3]. Another option is 3D printed custom made mega-prosthesis; 3D prosthesis design in a computer may achieve more volume and structural compatibility of the prosthesis [4]. Lastly, amputation consist the ultimate, unfortunate scenario [5]; while salvage of severely injured limbs remains our priority.

Nowadays, the usage of the prototyping technology of 3D printing has been gaining more and more popularity, as it permits the

* Corresponding author at: Orthopaedics, Democritus University of Thrace, University Hospital of Alexandroupolis, Dragana, 68100 Alexandroupoli, Greece.

E-mail address: iliopoulose@gmail.com (E. Iliopoulos).

https://doi.org/10.1016/j.tcr.2023.100848
Accepted 15 May 2023
Available online 16 May 2023

immediate manufacturing of custom-made implants, which can lead to detail preoperative planning of complicated surgical procedures [6]. Besides the key benefit of accurate preoperative planning, it has also the major advantage to foresee possible intraoperative difficulties, thus it may be considered as essential tool in our treatment quiver.

The aim of this study was to present an innovative treatment technique using 3D printing technology, in a case of septic non-union and chronic osteomyelitis of distal tibia.

Case report

A 66-year-old male patient was referred to our orthopaedic department with a painful septic non-union and chronic osteomyelitis of the left distal tibia, with frail and scared skin associated with a discharging sinus (Fig. 1). The patient was non-smoker, with a body mass index of 26.2 and without past medical history. A year earlier he had sustained an open fracture of the left distal tibia, which was treated in another medical center with initial wound debridement, open reduction and internal fixation, using a medial distal tibia plate and a distal fibula plate through a direct medial and lateral incisions and primary closure. Subsequently, the fracture site was complicated by infection and he was further treated with hardware removal, wound debridement, application of monolateral external fixator and long term antibiotics approximately 3 months after the initial procedure. A second wound debridement and washout was necessary 6 weeks later. The monolateral external fixator was removed about 5 months after the injury.

The patient underwent a thorough pre-operative assessment, including a computerized tomography (CT scan) and a Magnetic resonance imaging (MRI). The articular segment of the distal tibial (covering approximately 8 cm of the distal tibia) was deemed to be non-viable and the decision to remove the distal tibia was made. Instead of manually constructing a spacer, we preferred the construction and application of a patient specific custom-made spacer, which was the mirrored identical of the patient's normal right distal tibia. The reason behind this decision, was that with this way it would be possible to maintain the leg length and prevent the contracture of the soft tissue around the ankle, giving the patient a normal distal tibia and a stable ankle joint, avoiding further surgical intervention, due to the questionable viability of the local skin and the patient's choice for as minimum surgical interventions as possible as well. The option of debridement and application of a vascularized free flap was not evaluated as a safe option as the condition of the local arteries after the initial trauma and interventions was not adequate.

With that in mind, a radical surgical debridement was performed, which was involving the debridement of the affected soft tissues, and the removal of the infected bone leaving a bone defect of the distal tibia of 8 cm (as planned). Five tissue samples were obtained and send for microbial cultures. Furthermore, an antibiotic loaded with gentamicin & clindamycin cement spacer (Copal G + C, Heraeus Medical GmbH, Wehrheim, Germany) was implanted. The production of this spacer was achieved by 3D printing technology which is described in detail in the next section of the article. A plastic matrix mold of the distal tibia, consisting of two parts, was printed and then covered with medical vaseline loaded gauzes and vancomycin powder, so as to prevent the plastic from melting while cement solidifies (Fig. 2A). The two parts of the matrix mold were covered and tied tightly with tire-ups and wires. In addition, two drill holes were made and filled with reamers, from which later syndesmosis sutures (Syndesmosis TightRope Implant System, Arthrex GmbH, Munich, Germany) would be passed (Fig. 2B). Finally, the cement was injected alongside with the insertion of a Steinmann in order to be used as an intramedullary device to the tibia shaft (Fig. 2C). Even though the spacer fitted exactly, it did not allow for a tension-free closure, as we did not consider the shrinkage of the surrounding soft tissues due to chronic inflammation. Consequently, a readjustment was necessary and the edges of the spacer were trimmed with a saw, in order to decrease its volume. Afterwards, the Steinmann was covered with cement and the spacer was introduced (Fig. 2D). Two syndesmosis tight ropes were passed from the pre-

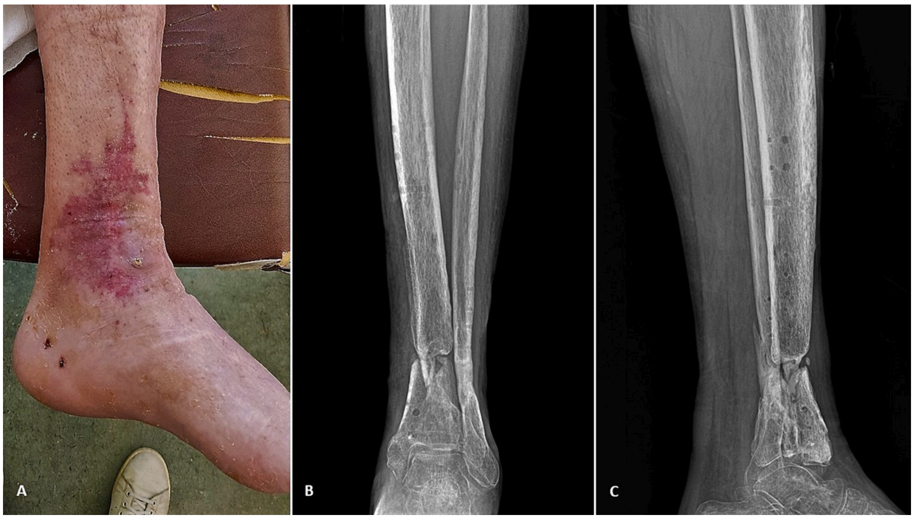

Fig. 1. Compromised soft tissue envelope of the affected left tibia with discharging sinus in the medial side of the ankle (A) and preoperative antero-posterior (B) and lateral radiographs (C).

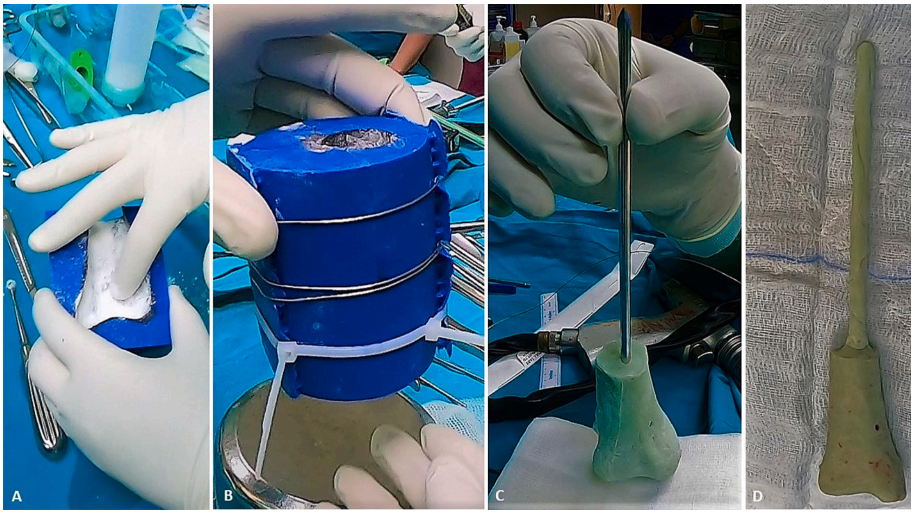

Fig. 2. Plastic mold of mirrored right tibia covered with Vancomycin powder (A), enclosed with tire-ups and wires (B) and then filled with cement alongside with the insertion of a Steinmann for the production of the spacer (C). The final construct after the necessary trimming, as the actual size was proven too large (D).

drilled holes, fixing the spacer with the distal fibula. The ankle joint was clinically stable in all stress tests intra-operatively. After skin closure, a bridging external fixation of the ankle was applied, and a negative pressure wound therapy to ensure an uneventful healing (Fig. 3).

Four out of five intraoperative tissue samples were positive for Staphylococcus Coagulase Negative which was treated with intravenous antibiotics, as per microbiology advice. By one month post-operatively the inflammatory markers were normalized, but despite that, the wound was constantly leaking through a small area at the distal part of the medial wound. The fluid was clear and aseptic, confirmed by multiple cultures. At this point the initial plan was abandoned and a further surgical intervention deemed necessary.

The second surgical intervention was performed approximately five weeks after the first one. Under general anesthesia, before the start of the procedure, after the removal of the external fixator, an evaluation of the stability of the ankle joint was performed under image intensifier. The ankle joint found to be stable in varus, valgus stress and at the external rotation stress. Anterior and posterior drawer stress tests were stable as well. The range of motion of the ankle joint was almost normal (25° of plantar flexion to 10° of dorsiflexion). After removal of the spacer, further surgical debridement was performed. The wound was closed primarily and an Ilizarov circular frame was applied. An osteotomy of the proximal tibia was performed and a standard distraction osteogenesis protocol

Fig. 3. An external fixator was placed to enhance the stability of the construct, as well as to allow for a primary closure of the surgical trauma in combination with a Negative Pressure Wound Therapy device (A). Post-operative radiographs depicting the filling of the bone defect from the custom-made spacer and the congruency of the 'recreated' ankle joint. Anteroposterior (B) and lateral views (C).

was followed using the ilizarov circular frame, with the view to fill the 8 cm bone defect (Fig. 4).

After 3 months of distraction osteogenesis the docking site had been reached and a docking site procedure performed. At this surgical intervention the previous lateral incision was used. The distal part of the fibula was removed and used as bone graft at the docking site. The proximal articular surface of the talus was removed and an ankle arthrodesis was achieved by using the existing Ilizarov circular frame. A minor shortening (<1 cm) was necessary to achieve good bone interposition (Fig. 5).

The patient was closely followed up in the outpatient's department allowing full-weight bearing through the frame construct. The wound healed uneventfully and approximately 4 months later, appropriate callus density had been obtained at the osteogenesis site and the arthrodesis had been completed leading (after dynamization) to removal of the circular frame. A Sarmiento cast was applied to support the mobilization of the patient for further 6 weeks after the frame removal. At the final follow up (6 months after the last procedure) the patient was walking pain free without the need of any walking aids. The use of a rocker bottom shoe was advised in order to improve his function (Fig. 6).

Scaffold report and design

To deal with the patient's needs a 3D model of the lower tibia was required for the replacement surgery. To do so three different construction stages where involved.

1. Segmentation phase
2. Virtual model phase
3. Physical printing phase

In the first phase a segmentation approach was conducted to isolate the geometry needed from the rest anatomy of the leg. The segmentation was based on the not affected side of the patient to guarantee a well geometrically formatted shape. In the second phase the isolated geometry was exported as a mesh to further be processed in order to avoid geometric incongruities. In addition, the mirrored geometry was generated to fit the needs of the virtual model. In the last phase the virtual model was constructed by implementing Additive Manufacturing (AM).

Segmentation phase of Tibia geometry

In order to create the scaffold, a "Digital Imaging and Communications in Medicine" (DICOM) data file retrieved from the CT scan of the patient was used. The CT scan was conducted on the unaffected leg of the patient from the distal femur to the toes. The CT data were acquired from a Philips CT Ingenuity 128 DS scanner with an X-ray tube. The X-ray tube's current was 206 mA. The resolution of the "DICOM" file was 0.336 mm × 0.336 mm × 1 mm, while the three-dimensional array of the data image was 814 × 246 × 2068 where 814 denotes the number of slices perpendicular to x axis (sagittal plane), 246 to y axis (coronal plane) and 2068 to the z axis respectively (axial plane). The slice thickness was 2 mm and the spacing between slices was 1 mm.

The target geometry was the lower part of the tibia bone extended approximately 10 cm from the base of talus bone. Since the DICOM file also includes complex anatomical details in order to remote the target geometry medical imaging processing ITK-SNAP 3.6 Software was used [7]. A region competition feature image was generated. As foreground, values in the greyscale range from 113.0 to

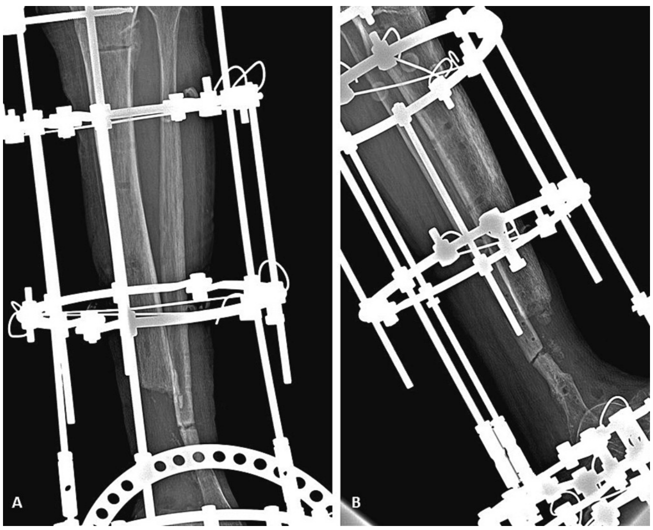

Fig. 4. Post-operative anteroposterior (A) and lateral (B) radiographs after removal of the spacer and proximal osteotomy of the tibia in the context of distraction osteogenesis procedure in order to fill the bone defect.

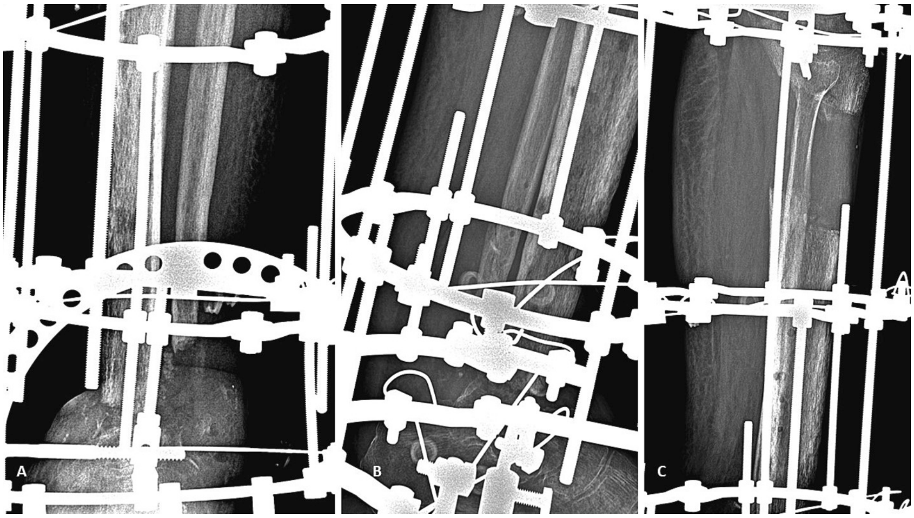

Fig. 5. Pre-operative plain radiographs before the ankle arthrodesis procedure. The a gap of approximately 1 cm at the docking site requiring a corresponding shortening. Anteroposterior (A) and lateral views (B). Distraction osteogenesis at consolidation phase (C).

Fig. 6. Clinical photograph of medial wound 6 months after the last operation (A). Plain radiographs of the ankle at 6 months after the arthrodesis. Anteroposterior (B) and lateral views (C). Anteroposterior radiographic view of the proximal tibia, showing consolidation of the distraction site (D).

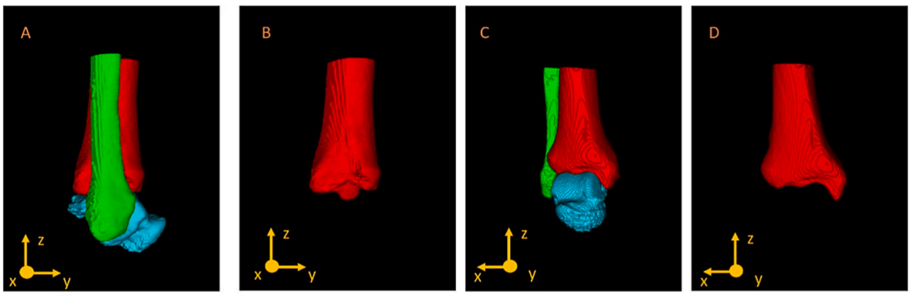

Fig. 7. 3D geometry of low leg anatomy in different planes (A,C). With red lower Tibia bone is represented, with green lower part of Fibula bone, while with green part of Talus bone. Fig. B,C isolate only the Tibia bone. (For interpretation of the references to color in this figure legend, the reader is referred to the web version of this article.)

1582 were used for the threshold filter tool. In a following step manual correction was implemented to further isolate the target segmented geometry. Fig. 7 shows the final segmentation of the lower Tibia bone (in red) as well as other bones in different colors and planes. Lastly the lower tibia geometry was exported as an ".stl" mesh file. The total facets of the mesh were 179,808.

Virtual model phase

As a following step the mesh file was imported in Fusion 360 Software [8] to further edit the mesh and convert it to solid body for the creation of the negative scaffold. The mesh initially was smoothed to avoid edges by a factor of 0.25 and then was reduced to 44,948 elements. The mesh was converted to solid, and the negative scaffold was generated as depicted in Fig. 8. The total volume of the bone was 8.2•10^(−2) m^3. Since the site of interest was the opposite side, a mirrored geometry had to be generated to fit the needs of the experiment.

Physical printing phase

As a final step the file was extracted as an ".obj" format and then a G-code was generated from the CraftWare software in order to print the object. The Fusion Deposition Modeling printing technique was applied. The print quality was set as high. The nozzle size of the printer was 0.8 mm, while the nozzle temperature and the bed temperature were 2500C and 1100C accordingly. The printing material was ABS and the printing time was approximately 8 h.

Discussion

3D printing is a promising technique for managing large bone defects after trauma. In the present case the application of the custom-made 3D printed cement spacer, did not fully succeeded as a final treatment for distal tibia septic non-union and chronic osteomyelitis with extensive bone lose. However, helped to manage the local infection and acted as a perfect spacer for the maintenance of the surrounding soft tissues. Managing these types of pathologies, can be really challenging even for experienced limb reconstruction experts, and the application of the 3D printing advances can be added to their toolbox.

Different techniques have been described in the literature for the treatment of extensive limb bone defects. Free vascularized fibular graft (FVFG) and bone transport (BT) using distraction osteogenesis are the most commonly utilized methods [1]. FVFG was not an appropriate choice for this case, as the state of the local arteries was not adequate due to initial trauma as well as the chronic infection. BT is well documented and constitutes the reference method for many surgeons when a reconstruction of a large bone defect is necessary [2]. Although in the end BT was performed, it was initially ruled out, due to patient's will to keep the surgical interventions to a minimum. Recently, induced membrane (IM) technique (Masquelet) has also been described as a reliable treatment method [3]. However, IM is based on a two-stage principle; hence, couple of surgeries would be required and for the same reason as with BT it was left out of consideration. 3D printed custom-made mega-prosthesis for the reconstruction of large bone defect, including the ankle joint, has been reported in the past, with good short-term clinical outcomes. A mega-prosthesis could be employed after a radical resection due to a bone tumor, but in this case, which involved an infection, it was a non-viable option [4]. Finally, amputation should be performed only as a last resort, when everything else has failed or the limb is beyond reconstruction [5].

3D printing in trauma

The 3D printing technology has been used previously in trauma for unilateral complex lower limb fractures. The unaffected limb was mirrored and a 3D model is produced and used for pre-operative planning and practice. This allowed the surgeons to use the unaffected limb as a reference to aid the reduction and plan the fixation with good results [6]. In pilon type distal tibia fractures, the use of 3D printing technology has been proven to be feasible as a pre-operative planning tool, reducing the surgical time and improving the achieved fracture reduction and clinical outcomes [7]. In this case the unaffected limb was also used as a reference for the 3D printing. However, a plastic mold was printed instead of the actual bone, as the purpose was to insert an antibiotic loaded spacer to deal with the infection as well as to replicate the distal tibia and the ankle joint.

3D printing in foot and ankle surgery

3D printing technology has regularly been used in foot and ankle surgery the last few years. The main use of this technology is in total talus replacements (isolated or combined with total ankle replacement) due to avascular talar necrosis. The contralateral unaffected talus is used as a reference for the implant printing. Metal implants are used normally for these procedures [8,9]. Plastic implants have been used previously in ankle fractures malunion for pre-operative planning, evaluation of the ankle joint defect and the accurate assessment of the potential bone graft needed [10]. Similar cases with persistent distal tibia nonunion have been treated previously with 3D printed titanium truss cages, as scaffolding for autologous iliac crest bone graft, leading to successful tibio-talo-calcaneal fusion with favorable clinical long-term results [11].

Sizing of implant

In the present case the size of the implant was mirrored identical of the contralateral side, and proven intraoperatively to be too

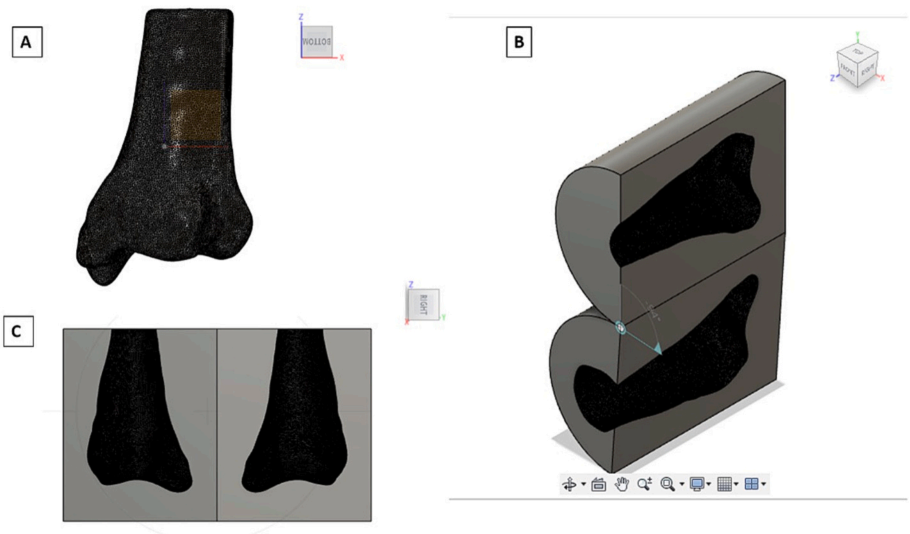

Fig. 8. The final mesh of the lower part Tibia bone (A) and the negative scaffold generated from it depicted in two different viewpoints (B,C).

large, occupying the defect, but not allowing a tension free closure, most likely due to the shrinkage/scarring of the surrounding soft tissues. Thus, the implant had to be trimmed using a surgical saw during the procedure. 3D printed implants used for other lower limb pathologies report mixed sizing techniques. Kadakia et al. report having three options of implant sizes available for total talus replacements due to avascular necrosis. The size of the implant was determined clinically during the operation based on the clinical stability, and usually the implant with actual size of the healthy talus was chosen [8].

This study is not free of limitations. Most importantly, it concerns a case report and therefore any generalization of the findings would be neither appropriate nor safe. Moreover, it should be mentioned, that even though the stability of the construct was ensured intra-operatively, the opportunity did not arise to test it clinically, while the spacer had to be removed preliminary due to adverse events already described. It is for the same reason, that long-term outcomes of this method could not be documented and are also lacking. However, in this study a novel application of 3D printing is described, for the management of extensile bone defects, that could prove especially useful in complex cases and thus warrants more future research.

Conclusions

3D printing technology advances the last years, provide us with more sophisticated and effective tools for managing complex orthopaedic pathologies. The present case report, provide valuable experiences on using these technologies in limb reconstruction. The use of a customized patient specific cement spacer for the management of persistent septic non-unions, is a promising option, that poses some challenges yet.

Declaration of competing interest

All the authors have nothing to declare.

Acknowledgements

The publication of the article in OA mode was financially supported in part by HEAL-Link.

References

[1] Ren G. Hong, R. Li, Y. Hu, Y. Chen, C. Chen, B. Yu, Treatment options for infected bone defects in the lower extremities: free vascularized fibular graft or Ilizarov bone transport? J. Orthop. Surg. Res. 15 (1) (2020 Dec 1) 1–11.
[2] M. Chaddha, D. Gulati, A.P. Singh, A.P. Singh, L. Maini, Management of massive posttraumatic bone defects in the lower limb with the Ilizarov technique, Acta Orthop. Belg. 76 (6) (2010 Dec 1) 811.
[3] P. Andrzejowski, A. Masquelet, P. Giannoudis, v., Induced membrane technique (Masquelet) for bone defects in the distal tibia, foot, and ankle: systematic review, case presentations, tips, and techniques, Foot Ankle Clin. 25 (2020) 537–586.
[4] D. Feng, J. He, C. Zhang, L. Wang, X. Gu, Y. Guo, 3D-printed prosthesis replacement for limb salvage after radical resection of an ameloblastoma in the tibia with 1 year of follow up: a case report, Yonsei Med. J. 60 (9) (2019) 882–886.
[5] J.F. Keating, A.H.R.W. Simpson, C.M. Robinson, The management of fractures with bone loss, JJBJS Br. 87 (2) (2005 Feb 1) 142–150.
[6] W. Zhang, Y. Ji, X. Wang, J. Liu, D. Li, Can the recovery of lower limb fractures be achieved by use of 3D printing mirror model? Injury. 48 (11) (2017) 2485–2495.

[7] W. Zheng, C. Chen, C. Zhang, Z. Tao, L. Cai, The feasibility of 3D printing technology on the treatment of pilon fracture and its effect on doctor-patient communication, Biomed. Res. Int. 18 (2018 Jan) 2018.
[8] R.J. Kadakia, C.C. Akoh, J. Chen, A. Sharma, S.G. Parekh, 3D printed total talus replacement for avascular necrosis of the talus, Foot Ankle Int. 41 (12) (2020) 1529–1536.
[9] C.C. Akoh, J. Chen, S.B. Adams, Total ankle total talus replacement using a 3D printed talus component: a case report, J. Foot Ankle Surg. 59 (6) (2020) 1306–1312.
[10] K. Horas, R. Hoffmann, M. Faulenbach, S.M. Heinz, A. Langheinrich, U. Schweigkofler, Advances in the preoperative planning of revision trauma surgery using 3D printing technology, J. Orthop. Trauma 34 (5) (2020) e181–e186.
[11] A.R. Hsu, J.K. Ellington, Patient-specific 3-dimensional printed titanium truss cage with tibiotalocalcaneal arthrodesis for salvage of persistent distal tibia nonunion, Foot Ankle Spec. 8 (6) (2015) 483–489.